Interaction of Superimposed Megaripples and Dunes in a Tidally Energetic Environment

Authors: Katie R. Jones, and Peter Traykovski
Source: Journal of Coastal Research, 35(5) : 948-958
Published By: Coastal Education and Research Foundation
URL: https://doi.org/10.2112/JCOASTRES-D-18-00084.1

Journal of Coastal Research	35	5	948–958	Coconut Creek, Florida	September 2019

Interaction of Superimposed Megaripples and Dunes in a Tidally Energetic Environment

Katie R. Jones[†] and Peter Traykovski[‡]*

[†]Massachusetts Institute of Technology–
Woods Hole Oceanographic Institution
Joint Program
Woods Hole, MA 02543, U.S.A.

[‡]Department of Applied Ocean Physics and Engineering
Woods Hole Oceanographic Institution
Woods Hole, MA 02543, U.S.A.

www.cerf-jcr.org

www.JCRonline.org

ABSTRACT

Jones, K.R. and Traykovski, P., 2019. Interaction of superimposed megaripples and dunes in a tidally energetic environment. *Journal of Coastal Research,* 35(5), 948–958. Coconut Creek (Florida), ISSN 0749-0208.

The superposition of smaller bedforms on larger dunes have been observed in multiple energetic tidal environments. This study analyzes the interaction of two scales of superimposed bedforms at Wasque Shoals, an ebb delta located approximately 1 km SE of Martha's Vineyard, Massachusetts. Data from a fixed rotary sidescan sonar deployed on a submerged quadpod captured the interaction of megaripples, or bedforms with wavelengths on the order of 1 m, with the lee side of a migrating dune with a wavelength of approximately 100 m. The net convergence of megaripples on the tidally dominant lee face of the dune suggests that the megaripples serve as an intermediate step between grain-scale transport processes and the large-scale dune migration. This conceptual model is quantitatively tested given observations of seabed elevation changes and dune migration rates. With this novel data set, two scales of bedforms were resolved on subtidal timescales, facilitating new insights into the dynamics of superimposed bedforms in tidal environments.

ADDITIONAL INDEX WORDS: *Compound bedforms, Martha's Vineyard, tidal asymmetry.*

INTRODUCTION

Subaqueous bedforms cover most of the nearshore seabed in energetic environments. Formed from the interaction of waves and currents with an erodible seabed, they range in scale from small ripples with wavelengths on the order of centimeters to ridges and dunes with wavelengths extending from meters to kilometers (Ashley, 1990; Dalrymple and Rhodes, 1995; Soulsby, 1997). The ability of bedforms to steer flow, influence seabed friction, and affect the transport of sediment makes understanding the dynamics of bedforms crucial to understanding the overall behavior of coastal systems (Ashley, 1990; Johnson, 1916; Nielsen, 1992).

Superimposed bedforms, where smaller bedforms exist on top of larger bedforms, are ubiquitous to nearshore, tidally energetic environments. Bedforms tend to scale with some combination of water depth, grain size, and flow velocity (Dalrymple and Rhodes, 1995). Therefore, the simultaneous existence of multiple scales of bedforms in a given location has given rise to several different theories for the existence of superimposed bedforms.

Two of these theories for the simultaneous existence of multiple scales of bedforms, derived largely from riverine observations, are equilibrium superposition and disequilibrium superposition. In disequilibrium superposition, large bedforms are hypothesized to be formed from large flood events or strong flows, whereas smaller bedforms form during less energetic periods. The different scaling hierarchies therefore act independently, only existing together because of the large response time of the dunes (Dalrymple and Rhodes, 1995, Myrow, Jerolmack, and Perron, 2018). Allen and Collinson (1974) concluded that only the smallest scale bedform is expected to be active at a given time where disequilibrium superposition was assumed to be the explanation for superimposed bedforms. In the other theory, equilibrium superposition, the reduced magnitude flow in the boundary layer of the dunes causes the formation of the smaller bedforms (Dalrymple and Rhodes, 1995). A numerical study of dune generation in agreement with equilibrium superposition observed smaller bedforms forming on the stoss side of large dunes because of a slight deflection of the dune stoss slope (Doré *et al.*, 2016). In both equilibrium and disequilibrium superposition, however, the smaller bedforms do not strongly influence the larger scale features.

While these theories on the existence of superimposed bedforms suggest that the multiple scales simply coexist, more recent studies have hypothesized that the different scales of bedforms interact, although this interaction is still poorly understood (Doré *et al.*, 2016). Off (1963) suggested a relation between sand waves and tidal current ridges should exist; however, from a lack of detailed surveys, this relation could not be quantified. Further work on tidal ridges similarly hypothesized that offshore tidal ridges are made from the accretion of cross-beds formed by dunes (Lobo, Maldonado, and Noormets, 2010; Reynaud and Dalrymple, 2012). More recently, Lefebvre, Ernstsen, and Winter (2013) suggested that smaller bedforms may be influencing the dunes on which they reside. Laboratory studies of superimposed bedforms in unidirectional flows indicated that the sediment transport of the smaller features may influence the sediment transport of the larger bedforms; however, this hypothesis was not quantitatively tested (Ven-

DOI: 10.2112/JCOASTRES-D-18-00084.1 received 15 January 2018; accepted in revision 21 March 2019; corrected proofs received 24 April 2019; published pre-print online 20 May 2019.
*Corresponding author: ptraykovski@whoi.edu

ditti, Church, and Bennett, 2005). Finally, numerical modeling studies on nonlinear bed development in a unidirectional flow show smaller bedforms migrating faster and eventually merging with the larger bedforms in the domain (Doré *et al.*, 2016). When there were superimposed bedforms on dunes, this study found that the superimposed bedforms eventually promoted the decaying of the dune crest (Doré *et al.*, 2016). Although these past studies hypothesize the interaction of the different scales of bedforms that make up a superimposed bedform, they lack the field data needed to quantify and validate this hypothesis.

In tidally energetic environments where the flow reverses direction, sediment transport might be sufficient for the smaller bedforms but not the larger bedforms to reverse their asymmetry and migration direction (Allen and Collinson, 1974; Bokuniewicz, Gordon, and Kastens, 1976). This results in a complex migration pattern, wherein the larger bedforms are slowly migrating in the direction of the dominant flow, while the smaller bedforms superimposed on them are migrating back and forth with the tides.

In addition to the tidally reversing flow, the presence of the larger bedforms may also affect the smaller bedform migration. In nearshore environments, the large height of bedforms relative to the water depth may significantly influence the surrounding flow and subsequent smaller bedform migration. The Bernoulli equation, which conserves energy, predicts flow acceleration over bedform crests given the shallower water depth. These larger velocities over the dune crests may influence the migration rate of the smaller bedforms as bedform migration is roughly proportional to U^3, where U is the free stream flow velocity (Fredsøe and Deigaard, 1992; Simons, Richardson, and Nordin, 1965). Additionally, when bedforms have a steep lee face, the flow may separate, forming a wake. This wake may result in the net migration of smaller features in the opposite direction of the free stream flow (Winter *et al.*, 2008). Therefore, the presence of a larger bedform may affect the migration rate of smaller superimposed bedforms.

In the work described in this manuscript, novel observational techniques were used to observe the migration rate of multiple scales of bedforms simultaneously, providing insight into the interaction of different scales of bedforms. The migration rate or response time in the case of bedform formation in a uniform flow and energetic conditions where the Shields parameter θ is greater than the critical Shields parameter is approximately proportional to U^3 and inversely proportional to bedform height h (Fredsøe and Deigaard, 1992; Simons, Richardson, and Nordin, 1965). For a given flow velocity U, larger bedforms will therefore migrate or respond at a slower rate than smaller bedforms (Perillo *et al.*, 2014). As a result of the differential migration rate or response time from bedform dynamics theory, the smaller megaripples superimposed on the dunes will consequently migrate or respond faster than the dunes on which they reside (Dalrymple, 1984; Dalrymple and Rhodes, 1995; Rubin and McCulloch, 1980).

The observations in this study, with high spatial and temporal resolution, were able to resolve a spatial variation in migration rate of the megaripples as a function of distance along the dunes. According to size-dependent bedform migration rate scaling, a new conceptual model on the interaction of multiple scales of bedforms in a tidally energetic environment is presented with sufficient observations to test the model quantitatively. This conceptual model suggests that smaller bedform migration serves as an intermediate step between grain-scale transport processes and larger scale bedform migration.

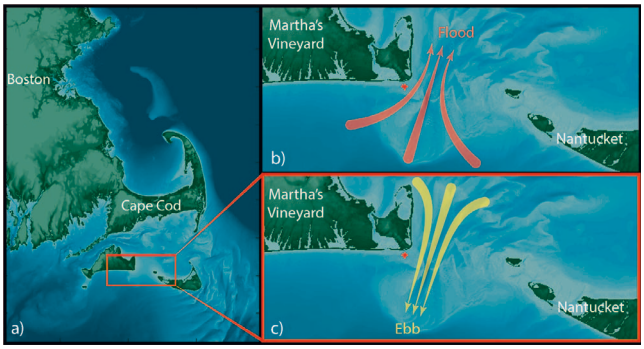

Figure 1. (a) National Oceanic and Atmospheric Administration coastal relief map of the east coast of Massachusetts. (b) Wasque Shoals is located off the SE corner of Martha's Vineyard, indicated by the red dot. During flood, water is funneled into the inlet between Martha's Vineyard and Nantucket. (c) During ebb, the water leaves Nantucket Sound as a jet, creating a flood-dominated flow at Wasque Shoals.

METHODS

Data of superimposed bedforms were obtained in the field by novel observational techniques.

Study Area

The measurements were conducted off the SE corner of Martha's Vineyard, Massachusetts, at Wasque Shoals (Figure 1). The flow in this region is tidally dominated and is funneled into the inlet between Martha's Vineyard and Nantucket during flood and shot out like a jet during ebb, similar to the idealized theory for horizontal tidal exchange through an inlet (Figure 1b,c; Stommel and Farmer, 1952). The study site is indicated by the red dot in Figure 1b,c, where the water depth is approximately 6 m. Given the horizontal tidal exchange pattern, the flow is asymmetric and flood dominated at the study site as the flow during ebb separates at the 90° corner in the coastline of SE Martha's Vineyard (Hopkins, Elgar, and Raubenheimer, 2017) and is thus reduced at the study site compared with the flood.

Instruments and Platforms

Previous methods to study seabed dynamics include ship-based or underwater frame platforms equipped with acoustic instruments. Single-beam echosounders have commonly been mounted on the hull of a ship to obtain bathymetry along the ship track. However, because of the limitations in cost, human fatigue, and time, these measurements are usually taken at a low temporal resolution and only provide depth information along one dimension. Sidescan sonar is another common instrument to observe the seabed, and because of their low cost, they can be mounted on either a ship or underwater frame

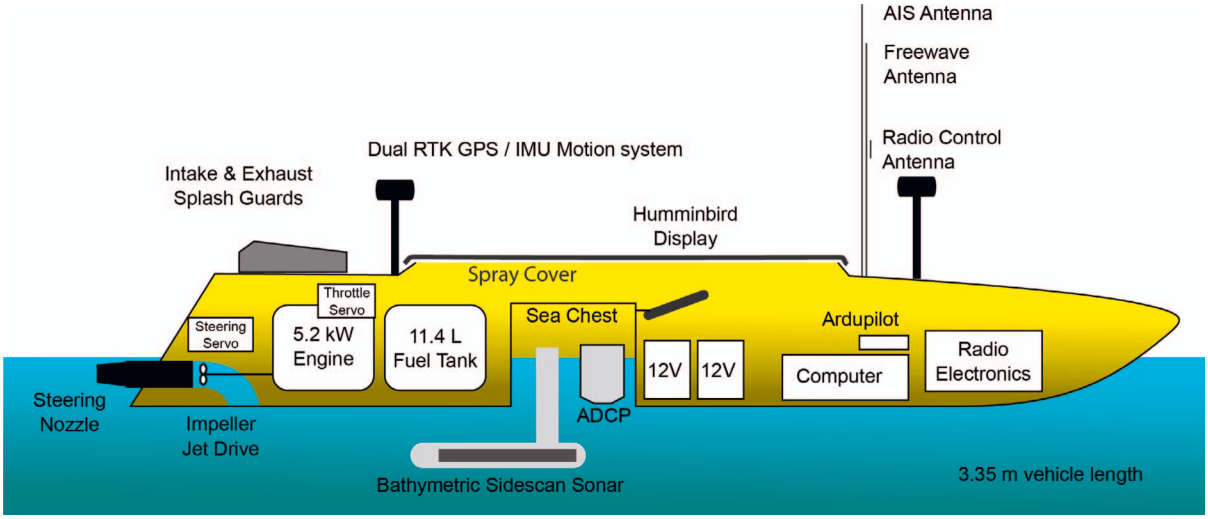

Figure 2. Autonomous jet-powered kayak, Jetyak, equipped with a bathymetric sidescan sonar, dual real-time kinematic (RTK) GNSS antennas, and a Nortek Signature 1000 ADCP. The Jetyak is jet-driven and powered by an air-breathing gas engine and has hybrid remote control/autonomous navigation capabilities.

on a rotary stepper motor (Irish *et al*., 1998). When mounted on a frame, sidescan sonar has the advantage of much higher temporal resolution (typically tens of minutes) compared with a ship (typically days) at the expense of reduced areal covered. The main drawback of sidescan sonar is they typically only provide backscatter intensity with no depth information. However, in situations with periodic bedforms, where several bedforms are resolved by the sidescan sonar, a technique was developed by Jones and Traykovski (2018) that uses the length of the acoustic shadows to estimate bedform height and asymmetry. Multibeam sonar can measure depth along a swath at discrete angular increments (Clarke, Mayer, and Wells, 1996). However, because of their expense and limited depth to swath width ratio, they are commonly mounted on a ship that has the same ship-based limitations as those described above.

Limitations in observational techniques has made it difficult to observe simultaneously the dynamics of multiple scales of bedforms on tidal timescales. Recent advances in both platforms and instrumentation are detailed below that can observe such bedforms.

Autonomous Jet Drive Kayak

An autonomous water jet drive kayak, referred to as a Jetyak, is a platform capable of collecting high-resolution data of the seabed and flow (Figure 2). The following information on the Jetyak specifications is from Kimball *et al*. (2014), and some aspects of the Jetyak have been updated for the measurements in this study. The Jetyak is jet propelled by a vector-steered water jet with a draft of 20 cm and an air-breathing and air-cooled gasoline engine. Given these features, the Jetyak can travel up to 5.5 m/s with 6 to 8 hours of endurance on a single gas tank, allowing it to operate in strong currents and shallow environments, which makes it an ideal platform for tidally energetic settings where superimposed bedforms are common. The steering and throttle of the Jetyak is controlled by a Pixhawk 2.1 autopilot, allowing the Jetyak to be pre-programmed to operate in an autonomous GPS waypoint following mode and accurately follow track-lines in strong cross-currents.

The Jetyak is equipped with instruments to measure both bathymetry and flow. The data analyzed in this manuscript came from two versions of the Jetyak. The first version had a Humminbird™ sidescan and single-beam echosounder, with which the Jetyak was able to obtain bathymetry along the trackline of the Jetyak. In subsequent surveys, the single-beam echosounder was replaced by a wide-swath bathymetric sonar, the Ping DSP 3DSS (3D sidescan sonar). The 3DSS is capable of measuring bathymetry in shallow environments with a greater than 10-cm horizontal resolution over a swath that is 10 times the water depth. The sonar operates at 450 kHz and uses patent pending computed angle of arrival transient imaging (CAATI) interferometry to compute the angle of the returned sonar signal from the target. The CAATI interferometry technique can distinguish between targets on the seafloor and in the water column that are at the same range. With the wide swath of the bathymetric sonar, the Jetyak attitude (pitch, heading, and roll) must be accurate and precise, because a slight change in attitude of the Jetyak would result in substantial changes in the horizontal and vertical location of the return pings from the bathymetric sonar. A dual-antenna postprocessing kinetic global navigation satellite system (GNSS) coupled with a NovAtel ADIS inertial motion unit was integrated on the Jetyak to form an altitude heading reference sensor (AHRS), which allows improved position accuracy of 2 to 5 cm and orientation to within 0.1°. With the accurate AHRS and 3DSS bathymetric sonar, the Jetyak is capable of simultaneously surveying bedforms that range in wavelength from 1 to 1000 m. In addition to the bathymetric sonar, both Jetyak versions were equipped with a downward-facing acoustic Doppler current profiler (ADCP) to measure the velocity throughout the water column. A Nortek Signature

Figure 3. Underwater quadpod placed on the seabed off the SE corner of Martha's Vineyard. The quadpod is equipped with multiple acoustic and pressure sensors to measure the seabed and local hydrodynamics.

1000 ADCP with 1-MHz frequency and broadband processing was configured to obtain measurements at a sampling rate of 4 Hz at 0.5-m bins vertically over a range of 10 m. The ADCP also collected bottom tracking data to remove the motion of the Jetyak from the flow velocity measurements.

Seafloor Frame

A seafloor frame equipped with acoustic instruments was deployed in the trough of a dune at Wasque Shoals at a water depth of approximately 6 m. The frame was deployed on 20 November 2013 and collected data until it was buried by a dune on 10 January 2014. The frame was equipped with an Imagenex 881L rotary sidescan sonar, which produced 40-m-diameter images of the backscattered intensity of the seabed at 4-cm resolution every 20 minutes (Figure 3). The high temporal and spatial resolution of a rotary sidescan sonar allows for multiple scales of bedforms to be observed simultaneously. In addition to rotary sidescan sonar, narrow-beam (~1°) multi-frequency (1, 2.5, and 5 MHz) acoustic backscatter sensors (ABSs) measured backscatter intensity profiles that resolve both boundary layer and seafloor. The ABS can obtain the local seabed elevation directly below the seafloor frame. In addition to these acoustic instruments that measure backscatter intensity, the flow velocity is commonly measured by acoustic instruments that utilize the Doppler effect. On the frames in this study, an Aquadopp current profiler measured the vertical velocity at 0.2-m bins over a range of 2 m. Finally, acoustic Doppler velocimeters (ADVs) measured the velocity and wave properties at a single point.

RESULTS

Superimposed bedforms were observed in the field by the observational techniques outlined above. For consistency in this manuscript, the term "dune" is used to refer to the large, 100-m-wavelength features whose height is a significant fraction of the water depth (Engelund and Fredsøe, 1982). The term "megaripple" is used to describe the approximately 1-

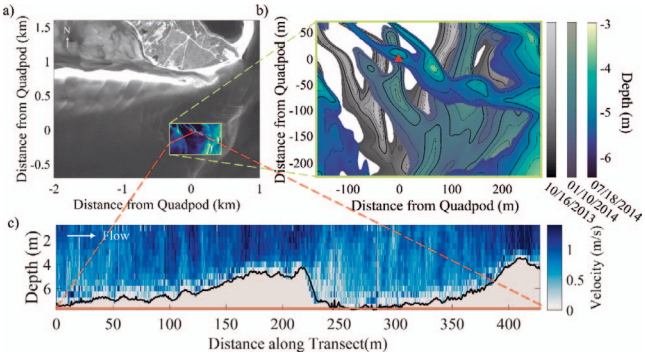

Figure 4. (a) The gray-scale image is a Pleiades satellite image taken on 22 July 2014 of the corner of Martha's Vineyard and Wasque Shoals and obtained from Airbus Defense and Space (2014). The color is bathymetry from a Jetyak survey with a single-beam echosounder taken on 18 July 2014. (b) Bathymetry from three Jetyak surveys over a 9-mo period with different color maps for each survey. The bedform bathymetry was contoured to a maximum depth of 5.5 m from the mean tidal elevation. The surface below 5.5 m, not shown, is relatively flat with a maximum depth around 6.5 m. The dunes are primarily migrating NE at a rate of 50 cm/d and rotating slightly in response to flood tide–dominated currents and waves from the SW. The triangle depicts the location of the quadpod that was buried by the *Y*-shaped dune on 10 January 2014. Up is north. (c) Transect of flow throughout the water column obtained from the ADCP on the Jetyak during flood. The flow is going from left to right, and a wake is present behind the dominant lee face of the dune.

m-wavelength bedforms superimposed on the dunes. Megaripples represent an intermediate scale of bedforms that are larger than typical ripples but do not occupy a significant fraction of the water depth, like dunes (Amos and King, 1984; Berne *et al.*, 1993; Boothroyd and Hubbard, 1975; Nielsen, 1992; Soulsby, 1997).

Dunes

Three bathymetric surveys were obtained from a single-beam echosounder equipped on the Jetyak taken over a 9-month period on 16 October 2013, 10 January 2014, and 18 July 2014. The survey covered a 400×800-m^2 area with tracklines spaced roughly 30 m apart. An interpolation scheme produced gridded bathymetry data that first computed intermediate interpolated tracklines and then applied an over-determined Laplacian partial differentiation equation solver (Li *et al.*, 2014). This technique is well suited for data with very high resolution along-track but much lower intertrack spacing and performs better than tradition interpolation schemes (kriging, *etc.*) in this sampling scenario. These surveys reveal dunes migrating to the NE, in the direction of flood, averaging 50 cm/d while rotating counterclockwise (Figure 4b). The *Y*-shaped dune in Figure 4b ended up burying the quadpod on 10 January 2014 and is the dune referenced in the data from the quadpod. Three to six months after burial, the quadpod was unburied as the dune continued to migrate NE, allowing recovery of sensors and data.

In all three surveys, the large dunes remained oriented toward the direction of flood, with the steep slope of the dune facing NE throughout the tidal cycle. Because the tidal flow reverses direction, the lee and stoss side of the dune also switch

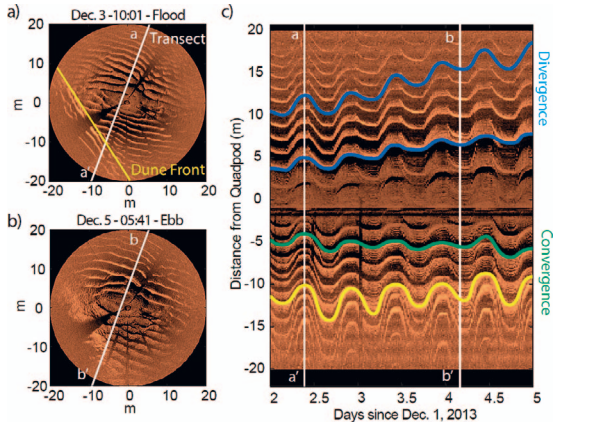

Figure 5. (a) Rotary sidescan sonar imagery during peak flood on 3 December 2013 at 1001 h. (b) Sonar imagery during peak ebb on 5 December 2013 at 0541 h. (c) Time stack of the intensity along a transect perpendicular to the megaripple crests and relative to distance from the quadpod. The blue-tracked megaripples depict the divergence of megaripples, and the green-tracked megaripple converges into the dune front, which is tracked in yellow.

throughout the tidal cycle. To distinguish between the two dune sides, the steep face is defined as the dominant lee face and the shallower dune slope as the dominant stoss face. The dunes have approximately a 7.5° dominant lee slope and 2° dominant stoss slope. These dune slopes measured by single-beam echosounder data are consistent with those measured by a high-resolution bathymetric sonar Jetyak survey taken in September 2016.

In addition to the single-beam echosounder, in the 2013 and 2014 surveys the Jetyak was equipped with an acoustic Doppler current profiler (ADCP) to measure the flow velocity at 0.5-m bins throughout the water column. The data from the ADCP show flow acceleration over the dune crests, along with a wake behind the steep dominant lee face during flood, but not behind the flatter subordinate lee face during ebb. Data depicting the wake during flood is shown in Figure 4c from a survey taken with the Jetyak on 18 July 2014. High-quality ADCP data from the ebb survey is not available because of larger waves during this survey. The noisy data suggests no separation during ebb tide when the flow is directed toward the steep face of the large-scale dunes. With similar superimposed bedform geometry and reversing tidal flows, Lefebvre, Ernstsen, and Winter (2013) show the presence of wake during flow aligned with dominant large-scale bedform direction and absence of wake during the reverse flow.

Megaripples

Imagery from the seafloor frame–mounted rotary sidescan sonar depict 1-m-wavelength megaripples superimposed on the *Y*-shaped dune (Figure 5a,b). These megaripples migrate and change asymmetry with the tides, as indicated by the length and position of their shadows (Jones and Traykovski, 2018). The megaripple wavelength and plan view orientation were computed from edge detection and spectral analysis techniques, resulting in wavelengths ranging from 0.5 to 3 m and oriented approximately 20° clockwise from the north.

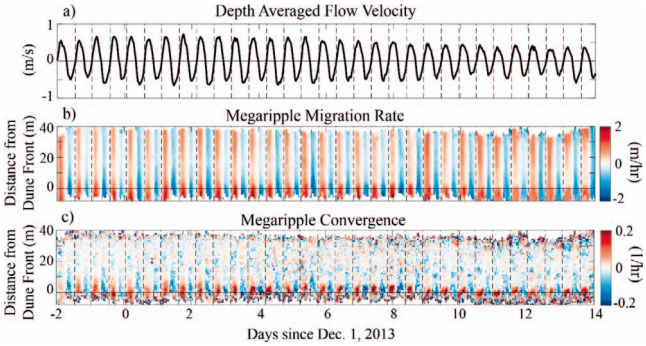

Figure 6. (a) Depth-averaged velocity from the Aquadopp mounted on the seafloor frame. The black vertical dashed lines represent the upward zero crossing used to define a tidal cycle. Positive numbers indicate flood tide, when the flow is going toward the N-NE. (b) Megaripple migration rate with respect to distance from the dune front averaged over seven transects perpendicular to the bedform crests and binned at 1 m. Positive values indicate megaripple migrating in the direction of flood. (c) Megaripple convergence with respect to distance from the dune front for a 16-d period.

To visualize the migration of the megaripples, time series of backscatter intensity profiles along a transect perpendicular to the megaripple crests are shown in Figure 5c. This time series depicts the tidal migration of the megaripples, resulting in the oscillatory signal of the megaripple crests with a period of approximately 12.4 hours. In addition to the megaripples migrating back and forth with the tides, a net component of the megaripple migration is dependent on the location of the megaripples on the dune, as well, that can be visually seen by tracking individual megaripples in the time series of Figure 5c. In this figure, the dune front, or lower edge of the dominant lee face, is defined as the location where the megaripple plan view orientation changes and the backscatter intensity is large, which is indicative of a surface facing the sonar. In the trough of the dune, NE of the dune front, the megaripples move in the net direction of flood and diverge, which is demonstrated by the two megaripples tracked in blue (Figure 5c). Close to the dune front, the megaripples migrate in the net direction of ebb, which is indicated by the green-tracked megaripple (Figure 5c). These megaripples also converge with the dune front (yellow line), which is slowly migrating in the direction of flood.

To quantify these spatial variations in megaripple migration tracked by individual features and to average over several megaripples, the following procedure was used. The migration rate of the megaripples was computed from the backscatter intensity obtained from the rotary sidescan sonar over a 16-day period from 27 November 2013 to 15 December 2013 when there were no large wave events. This approximately fortnightly period starts on a neap tide, contains a spring tide, and transitions back to neap (Figure 6a). Seven transects approximately 2 m apart were taken perpendicular to the megaripple crests and stacked in time, similar to Figure 5c. Megaripple features were then identified by peaks in the backscatter intensity gradient, with the megaripple migration rate computed from the change in megaripple crest and trough locations between time steps. The component of the megaripple migration rate in a coordinate system perpendicular to the

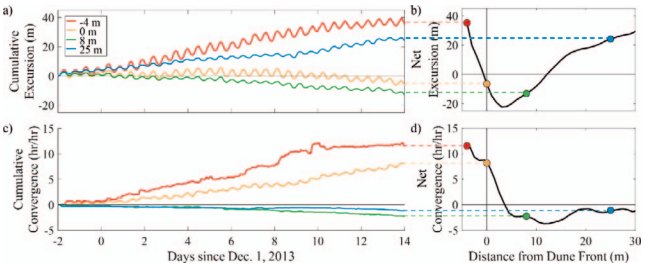

Figure 7. (a) Megaripple cumulative excursion over a 16-d period at four locations –4, 0, 8, and 25 m from the dune front. Positive excursion indicates megaripple migration in the direction of flood, or toward the N-NE, whereas negative excursion indicates migration in the direction of ebb. (b) Net megaripple excursion after 16 d. (c) Megaripple cumulative convergence for the same four locations as in panel (a). The convergence was calculated from a central difference of the gridded migration rates in a coordinate system locked to the dune front. (d) Net megaripple convergence. Units in panels (c) and (d) are hours per hour (h/h) from the time integration of convergence

dune front was binned at 1 m with respect to the dune front, where the dune front was defined for each tidal cycle by the location along the transect where the megaripples changed orientation (Figure 5a). The megaripple migration rate averaged over seven transects parallel to those shown in Figure 5a,b and spaced 2 m apart is shown in Figure 6b, which depicts the tidal signal in the megaripple migration rate. Differentiating the megaripple migration rate (Figure 6b) with respect to distance from the dune front results in megaripple convergence (Figure 6c).

Although the data of megaripple migration rate and convergence have a strong tidal signal (Figure 6b,c), the net megaripple excursion and convergence can be calculated by integrating each horizontal bin in time. Figure 7a depicts the cumulative megaripple excursion at four locations along the dune, –4, 0, 8, and 25 m with respect to the dune front, over the period 27 November 2013 to 15 December 2013 (16 days). The megaripple excursion at –4 and 25 m have a positive excursion, indicating net migration in the direction of flood, whereas the bins at the dune front and 8 m from the dune front have a net negative, or ebb, migration. The net megaripple excursion for each bin along the dune as shown in Figure 7b depicts a positive net megaripple migration everywhere except between the dune front and approximately 12 m from the dune front. The convergence was similarly temporally integrated with the cumulative convergence at –4, 0, 8, and 25 m from the dune front (Figure 7c) and the net megaripple convergence between –5 and 30 m from the dune front (Figure 7d). This convergence pattern results in megaripple convergence along the dominant lee face of the dune (roughly 4 m from the dune front) and divergence between 4 and 30 m from the dune front.

For statistical purposes, the megaripple migration rate and convergence (Figure 6b,c) was tidally averaged for each horizontal bin in a reference frame relative to the dune front with a tidal cycle defined by the upward zero crossing in the depth-averaged velocity (Figure 6a). This results in 32 estimates of the megaripple migration rate and convergence given the 16 days under consideration. The average and

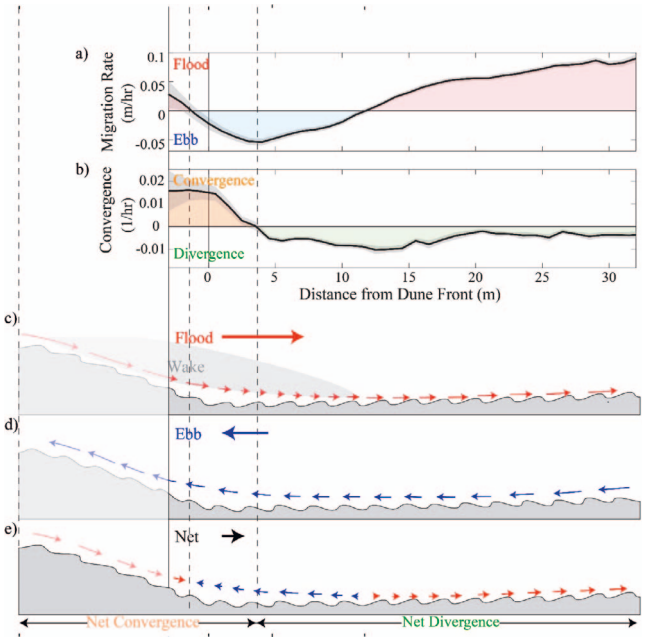

Figure 8. (a) Temporally averaged megaripple velocity over a 16-d period in a coordinate system relative to distance from the dune front. The gray-shaded region is the standard error of the number of bins included in the average from both different tidal periods and different transects. (b) Temporally averaged convergence obtained by differentiating the megaripple migration rate. (c–e) Schematic of the superposition of megaripples on the dune and their migration and asymmetry during flood (c) and ebb (d) tides. The faded region on the left was not directly observed because of the limited field of view of the rotary sonar system.

standard error of these 32 estimates was obtained (Figure 8a,b), resulting in a similar pattern in the net megaripple excursion and convergence depicted in Figure 7b,d.

DISCUSSION

The observations of megaripple convergence at the dune front motivated the development of a conceptual model relating the interaction of the two different scale features. This conceptual model is based on principles of bedform migration and was quantitatively tested with the observations of seabed elevation changes and dune migration rates.

Principles of Bedform Migration

In the presence of a current, bedforms typically migrate in the direction of the flow as sediment moves up the stoss side of the bedform, reaches the crest, and is then deposited on the downstream face (Simons, Richardson, and Nordin, 1965). The change in seabed elevation η at a given location from the convergence of sediment flux from bedform migration can be determined by the conservation of sediment mass and is commonly referred to as the one-dimensional Exner equation (Exner, 1920):

$$\frac{\partial \eta}{\partial t} = \frac{1}{(1-n)} \frac{\partial q_b}{\partial x} \quad (1)$$

where, n is the sediment porosity and is approximately equal to

0.3, q_b is the bedload sediment transport rate, x is distance in a parallel direction to the flow, and t is time. For a given position on the bedform ζ (*e.g.*, the location of the bedform crest), the location x of that position at a later time can be determined by the transformation in Equation (2) given a constant bedform migration rate a (Simons, Richardson, and Nordin, 1965):

$$\zeta = x - at \tag{2}$$

Using the transformation in Equation (2), the change in seabed elevation can be expressed in terms of bedform migration and bedform slope:

$$\frac{\partial \eta}{\partial t} = \frac{\partial \eta}{\partial \zeta}\frac{\partial \zeta}{\partial t} = -\frac{\partial \eta}{\partial \zeta}a \tag{3}$$

Equation (3) is also known as the kinetic equation and assumes the uniform migration of bedforms a, with no sediment bypassing from one bedform to the next (Berg, 1987; Engel and Lau, 1981; Hoekstra *et al*., 2004; Ten Brinke, Wilbers, and Wesseling, 1999).

Although the bedload transport rate q_b is commonly estimated from empirical equations, such as the Meyer-Peter and Müller formula, the bedload transport rate associated with bedform migration can also be estimated from the Exner equation (Equation [1]). The partial derivative of q_b with respect to x in Equation (1) can be replaced as follows given the partial derivative of ζ with respect to x in Equation (2):

$$\frac{\partial q_b}{\partial x} = \frac{\partial q_b}{\partial \zeta}\frac{\partial \zeta}{\partial x} = \frac{\partial q_b}{\partial \zeta} \tag{4}$$

Substituting Equations (3) and (4) into Equation (1) results in the following differential equation with respect to distance along bedform ζ:

$$\frac{\partial q_b}{\partial \zeta} = -\frac{\partial \eta}{\partial \zeta}a(1-n) \tag{5}$$

Integrating Equation (5) across a bedform with respect to ζ produces the average bedload sediment transport rate over the whole bedform $[q_b] = -[\eta]a(1-n) + c$, where the square brackets $[y] = 1/\zeta \int_x^{x+\zeta} y\, d\zeta$ indicate a spatial average of a given variable y over a bedform, and c is a constant of integration. For triangular bedforms, $[\eta] = 0.5h$, where h is the height of a bedform. Additionally, at the threshold of motion, $c = 0$ as $q_b = 0$. If the seabed is covered by bedforms with no bypassing of sediment from one bedform to the next, c will remain 0 and the equation for bedload transport averaged over a bedform can be simplified as shown in Equation (6) (Simons, Richardson, and Nordin, 1965):

$$[q_b] = -\frac{h}{2}a(1-n) \tag{6}$$

For energetic conditions where the Shields parameter θ is significantly greater than the critical Shields parameter, the bedload transport rate q_b is proportional to U^3. Therefore, the bedform migration rate a is proportional to U^3 and inversely proportional to bedform height h (Equation [6]). For a given flow velocity U, larger bedforms will therefore migrate at a slower rate than smaller bedforms. As a result of the differential migration rate from bedform migration theory, the smaller megaripples consequently migrate faster than the dunes on which they are superimposed (Dalrymple, 1984; Dalrymple and Rhodes, 1995).

Megaripple and Dune Interaction Conceptual Model

A conceptual model relating the two scales of bedform features was developed from the principles of bedform migration. From conservation of mass, assuming no sediment bypassing and that megaripples consist entirely of mobile sediment, the convergence of megaripples will result in an accumulation of sediment and subsequent increase in seabed elevation, and the divergence of megaripples will result in a decrease in seabed elevation. Because the convergence zone extends slightly past the dune front, the dune is expected to migrate slowly in the direction of flood as sediment is accumulated in front of the dune, thereby creating a two-way interaction between the bedform scales.

The megaripple convergence pattern can be attributed to the asymmetric, flood-dominated tide and flood-oriented dune as depicted in Figure 8c–e. The flood-dominated tide results in the majority of the megaripples having a net migration in the direction of flood. However, because the dune also remains flood oriented, it is in temporal disequilibrium with the flow during ebb, resulting in the presence of a wake during flood but no wake during ebb (Figure 4). Although measurements of small-scale bedform migration were only obtained on part of the dominant lee face because of the location of the frame relative to the dune, theory suggests that there would be a strong convergence of megaripples on the entire dominant lee side because of the separation of flow near the crest and subsequent wake during flood. Downstream of the dominant lee face, where there are measurements, the megaripple migration slows because of the weaker near-bed velocity in the wake of the dune, leading to strong convergence of megaripple migration on or just downstream of the lee slope. Further downstream, outside of the wake where the flow reattaches, the megaripple migration begins to accelerate, leading to divergence. On ebb, near the dune front where measurements are available. the megaripple migration is weakly divergent. Farther up the steep face, theory suggests that a balance between flow acceleration toward the crest would lead to divergence and gravity would lead to convergence, resulting in weak convergence or divergence, depending on which process dominates. Combining the megaripple convergence during flood and ebb results in a net migration with a convergence pattern on the lee face of the dune and divergence in the trough and upstream portions of the dominant stoss face (Figure 8e). This pattern results in the accumulation of sediment on the lee face of the dune and erosion of sediment near the trough. These locations of sediment erosion and deposition result in the net migration of the dune in the dominant flow direction.

To test quantitatively the conceptual model that the megaripples are driving dune migration with observations, both the change in seabed elevation and the dune migration rate were predicted from megaripple convergence and compared with direct measurements of these quantities from other instruments. These comparisons provide two partially independent tests of the concept that the megaripple convergence is driving dune-scale processes and are considered partially

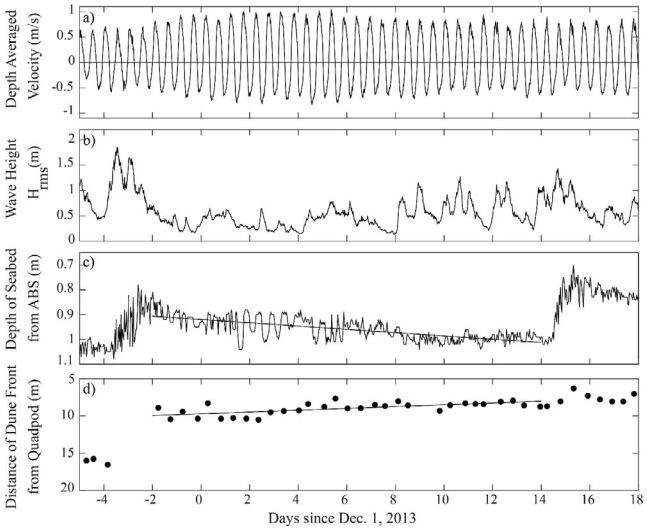

Figure 9. (a) Depth-averaged flow velocity from the Aquadopp current profiler located at the quadpod. (b) Root mean square (rms) wave height computed from ADVs on the quadpod. (c) Depth of the seabed measured from the ABS with a linear fit during 16 d of no large wave events. (d) The distance of the dune front from the quadpod where the ABS was located with a linear fit over 16 d with no large wave events.

independent because they use similar assumptions about megaripple and dune interactions, but different measurement methods. In the "change in seabed elevation" test the megaripple convergence is used to calculate dune-scale temporal changes in seabed elevation and is compared with a direct measurement of temporal changes in seabed elevation from the quadpod-mounted downward-aimed ABS echosounder. In the "dune migration" test, the temporal changes in seabed elevation calculated from megaripple convergence are used to estimate the dune migration rate and compared with a direct measurement of the dune migration rate from the location of the dune in the rotary sidescan sonar imagery.

Change in Seabed Elevation

The change in seabed elevation over time was directly observed from an ABS located on a tripod (Figure 3). Figure 9c depicts the depth of the seabed from the ABS from 27 November 2013 until 19 December 2013. During most of this time period the seabed elevation deceased slightly with time; however, during two periods of large wave events and flood tidal flows, the seabed elevation increased rapidly. Therefore, although the sudden increases in seabed elevation can be attributed to large wave events, the seabed elevation slowly decreases during periods of tidally dominated forcing with small waves. The change in seabed elevation estimated by linear regression was –0.66 ± 0.06 cm/d (95% confidence interval) over a 16-day period of no large wave events (Figure 9). This linear regression averages over tidal time scale megaripple migration processes but resolves the longer time scale and dune spatial scale processes. This 16-day period was also chosen because it is the period used for the megaripple migration rate (Figure 6b). The decrease in seabed elevation at the quadpod is expected because it is located on the dominant stoss side of a subsequent dune. Therefore, as the trough of the *Y*-shape dune migrates toward the quadpod, the quadpod observes a decrease in seabed elevation.

In addition to the direct measurement of seabed elevation with time, the change in seabed elevation can also be estimated given the conservation of mass through the one-dimensional Exner equation (Equation [1]) and the spatially averaged bedload transport rate over a megaripple (Equation [6]). For these calculations megaripple migration is used to estimate bedload transport. Substituting Equation (6) into Equation (1) results in Equation (7) for the change in seabed elevation, where h is the height of the megaripples and a_m is the migration rate of the megaripples:

$$\frac{\partial \eta}{\partial t} = -\frac{h}{2}\frac{\partial a_m}{\partial x} \tag{7}$$

To consider the net effect of megaripple migration, Equation (7) was first averaged over each tidal cycle, where T is approximately 12.42 hours, which is the length of a tidal cycle. A time series of d days long will yield $n = 24d/T$ estimates of the tidally average change in seabed elevation. These n estimates are then averaged together for each horizontal bin in a coordinate system reference to the dune front for each tidal cycle (Equation [8]):

$$\overline{\frac{\partial \eta}{\partial t}} = -\frac{1}{n}\sum_{n}\frac{h}{2}\frac{1}{T}\int_0^T \frac{\partial a_m}{\partial x}dt \tag{8}$$

These n estimates are also used to calculated statistics such as standard errors to estimate error bounds. The dune front spatial referencing does not vary within an individual tidal cycle but does follow the dune migration on a subtidal time scale, thus requiring double averaging in Equation (8).

The temporal mean of the megaripple height of 0.1 m was estimated on the basis of a megaripple aspect ratio h/λ of 0.1, obtained by applying the method outlined in Jones and Traykovski (2018) to the rotary sidescan sonar data. The tidally averaged megaripple convergence on the right-hand side of Equation (8) can be estimated from megaripple migration rates, as shown in Figures 7d and 8b. Because the megaripple convergence varies spatially with location on the dune, convergence was calculated at the location of the quadpod, since this is where the change in seabed elevation from the ABS is estimated. During the 16-day time period where the change in seabed elevation was directly estimated from the ABS and the megaripple convergence was computed, the dune front was approximately 8 m from the quadpod (Figure 9d). The net convergence of the megaripples 8 m from the dune front was –0.0059 ± 0.002 hr^{-1} (95% confidence interval) (Figure 8b). Multiplying by $h/2$, assuming a triangular bedform, results in a change in seabed height estimated from Equation (8) of –0.71 ± 0.25 cm/d (95% confidence interval). Because the convergence is relatively constant during this time period (Figure 7c yellow line), the product of the temporal mean of the convergence rate with the temporal mean megaripple height gives an accurate estimate of predicted elevation change from the convergence.

Table 1. *Estimate of the change in seabed elevation with time obtained directly from the ABS and indirectly from megaripple convergence.*

Estimated Method	$\partial\eta/\partial t$ (cm/d)	95% CI
Direct	−0.66	0.06
Predicted	−0.71	0.25

CI = confidence interval

The estimated change in seabed elevation from the convergence of megaripples (–0.71 ± 0.25 cm/d) has overlapping error bounds with the seabed elevation change computed directly from the ABS (–0.66 ± 0.06 cm/d), with a percent difference in the mean of 7.3% (Table 1). This result suggests that megaripple convergence could be the mechanism that directly forces dune-scale elevation changes.

Dune Migration

The conceptual model that megaripples serve as an intermediate step in dune migration can be further quantitatively examined from the dune migration rate. The migration of the dune during a period with tidally dominated forcing can be directly estimated by measuring the distance of the dune front to the quadpod using rotary sidescan sonar data. A dune migration rate of 12 ± 3.6 cm/d (95% confidence interval) is estimated from a linear regression of the distance of the dune front from the quadpod (Figure 9d).

The dune migration rate can also be estimated from the convergence of the megaripples given the kinetic equation that assumes dune movement at a constant velocity without changing shape and no sediment bypassing (Equation [3]). Temporally averaging Equation (3) results in the following equation for the average dune migration rate a_d:

$$\overline{a_d} = -\frac{\overline{\partial\eta/\partial t}}{\overline{\partial\eta/\partial\zeta}} \tag{9}$$

Because the dune migrates a very small distance (∼0.5 m) over a tidal cycle compared with the bedform size (∼100 m), the temporally averaged dune slope $\overline{\partial\eta/\partial\zeta}$ can be assumed to be constant. The dune front is defined by the high backscatter intensity from the seabed and the change in megaripple orientation, which is hypothesized to be due to the steep dominant lee face of the dune. From the Jetyak survey with an echosounder taken on 16 October 2013, the slope at the dune front is estimated to be $\overline{\partial\eta/\partial\zeta} = -0.13$, with a maximum dominant lee face slope of –0.18 and slope at the transition from a gradual slope to steep slope of –0.07. The average change in bed elevation from megaripple convergence (numerator of right side of Equation [9], $\overline{\partial\eta/\partial t}$) can be estimated from the tidally averaged Exner equation, Equation (8). In the above section, the change in bed elevation from megaripple convergence at the quadpod (8 m from the dune front) was approximately –0.71 cm/d, whereas the average change in bed elevation at the dune front is predicted to be 1.8 ± 0.7∼cm/d (95% confidence interval) based on a convergence of 0.015 ± 0.006 hr^{-1}. This results in a dune migration rate of 13.8 ± 5.5 cm/d (Equation [9]).

The average migration rate obtained from the quotient $\overline{\partial\eta/\partial t}$ calculated from megaripple convergence with the dune lee side slope $\overline{\partial\eta/\partial\zeta}$ (13.8 ± 5.5 cm/d) is within the 95% confidence interval of the dune migration rate obtained directly from the observations (12 ± 3.6 cm/d) with a percent difference in the mean of 13.9% (Table 2). In addition to the analysis showing that dune-scale elevation changes can be predicted from megaripple convergence, this analysis provides an independent second test that megaripple convergence may be driving dune migration.

Table 2. *Estimate of dune migration obtained directly from the location of the dune with the rotary sidescan sonar and indirectly from the convergence of megaripples.*

Estimated Method	$\overline{a_d}$ (cm/d)	95% CI
Direct	12.0	3.6
Predicted	13.8	5.5

CI = confidence interval

The assumption of no bypassing is not a strict condition because equal bypassing at both large and small scales would lead to similar results. Analysis of observations over large ($\lambda \sim$ 50 m, $h \sim$ 2 m) dunes in unidirectional riverine flow by Kostachuk (2008) indicated that about 17% of the total suspended load was deposited on the lee side of the dune but did not indicate the ratio of bedload to suspended load and relative contributions to dune migration. In the case of superimposed bedforms considered here, suspended sediment that bypassed the megaripples but converged on the larger dune scale would lead to larger dune migration than predicted by megaripple convergence, which is not consistent with the analysis.

CONCLUSIONS

This study proposes a conceptual model whereby the convergence of tidally reversing megaripple migration acts as an intermediate step between grain-scale movement and larger scale unidirectional dune migration. Past work on bedform dynamics attributes the migration of bedforms to individual sediment grains moving up the stoss side of a bedform, reaching the crest, and avalanching into the trough (Engelund and Fredsøe, 1982; Nielsen, 1992; Simons, Richardson, and Nordin, 1965). Although this process is still believed to drive the smaller megaripple migration, the conceptual model presented in this manuscript proposes that when multiple-scale bedforms are superimposed, the migration of the larger scale bedforms is directly forced by the smaller superimposed bedforms. The analysis of measurements presented in this manuscript do not prove that this conceptual model is valid but do provide a necessary condition for the model to be valid. To provide absolute proof that the model is valid, the entire sediment budget would need to be closed with measurements of all transport processed (bedload and suspended load) over an entire large-scale bedform over a time sufficient for substantial migration to occur.

Furthermore, this conceptual model provides an alternative interpretation of the role superimposed bedforms to two prior conceptual models: equilibrium superposition and disequilibrium superposition. Disequilibrium superposition suggests that only one scale of bedform can be active at a given time and the different scales are formed from different processes, such as a large flood. In this case, different scales of bedforms

coexist but do not interact. In equilibrium superposition, the smaller scales are formed within the boundary layer of the larger bedforms. In this case, the larger bedforms influence the smaller features through formation of large-scale boundary layers; however, the smaller bedforms only weakly influence the larger features through the modification of the inner boundary layer structure. The conceptual model presented here and the equilibrium theory share the common feature that the structure of the larger scale boundary layer is essential for controlling the dynamics of the small-scale bedforms. The separation in the lee of the large dunes creates the reduced migration rates of smaller bedforms that force large-scale convergences. However, the conceptual model presented here contains explicit forcing of the large-scale convergences by small-scale bedform migration, which was not explicitly described in the equilibrium theory.

The conceptual model presented from this work is based on tidally dominated flows with minimal wave energy. Large wave events, however, are substantial to dune dynamics; the average dune migration rate over a 9-month period obtained from Jetyak surveys is approximately 50 cm/d, roughly five times as large as the dune migration rate estimated from megaripple convergence. During storms, large amounts of sediment are suspended, and the dune migrates far, as indicated by the large change in both seabed elevation from the ABS and the distance of the dune front from the quadpod. It is speculated that the direction of the waves, the timing of large wave events relative to tidal phase, and the intensity of the wave event can all contribute to the migration of the dunes and alteration of the seafloor bathymetry. Understanding the large wave events and the subsequent suspended sediment is crucial in the overall migration and morphodynamics of the larger dunes in environments with episodic large waves such as Wasque Shoals. However, in environments with smaller waves and tidally dominated bedform migration processes, this new conceptual model may describe the dynamics of the interaction of smaller megaripples with larger dunes.

ACKNOWLEDGMENTS

We thank Kevin Manganini, Jay Sisson, Andy Girard, Benjamin Jones, the students and postdocs in the Coastal Ocean Fluid Dynamics Laboratory, and the Woods Hole Oceanographic Institution staff for their assistance. This project is partially supported by the National Science Foundation through a Graduate Research Fellowship and a Massachusetts Institute of Technology (MIT) Energy Initiative Fellowship. Additionally, funding for field work and analysis was obtained from National Science Foundation grants OCE-1634481 and OCE-1635151, Strategic Environmental Research and Development Program grants W912HQ-13C-0044 (project MR-2319) and W912HQ17C0012 (project MR-2729), and Office of Naval Research grants N00014-06-10329 and N00014-13-1-0364.

LITERATURE CITED

Airbus Defense and Space, 2014. *Satellite data*. https://www.intelligence-airbusds.com/satellite-data/

Allen, J. and Collinson, J., 1974. The superimposition and classification of dunes formed by unidirectional aqueous flows. *Sedimentary Geology*, 12(3), 169–178.

Amos, C. and King, E., 1984. Bedforms of the Canadian Eastern Seaboard: A comparison with global occurrences. *Marine Geology*, 57(1–4), 167–208.

Ashley, G.M., 1990. Classification of large-scale subaqueous bedforms; a new look at an old problem. *Journal of Sedimentary Research*, 60(1), 160–172.

Berg, J.H., 1987. Bedform migration and bed-load transport in some rivers and tidal environments. *Sedimentology*, 34(4), 681–698.

Berne, S.; Castaing, P.; Le Drezen, E., and Lericolais, G., 1993. Morphology, internal structure, and reversal of asymmetry of large subtidal dunes in the entrance to Gironde estuary (France). *Journal of Sedimentary Research*, 63(5), 780–793.

Bokuniewicz, H.; Gordon, R., and Kastens, K., 1976. Form and migration of sand waves in a large estuary, Long Island Sound. *Marine Geology*, 24(3), 185–199.

Boothroyd, J.C. and Hubbard, D.K., 1975. Genesis of bedforms in mesotidal estuaries. *In:* Cronin, L.E. (ed.), *Geology and Engineering*. New York: Academic Press, pp. 217–234.

Clarke, J.E.H.; Mayer, L.A., and Wells, D.E., 1996. Shallow-water imaging multibeam sonars: A new tool for investigating seafloor processes in the coastal zone and on the continental shelf. *Marine Geophysical Researches*, 18(6), 607–629.

Dalrymple, R.W., 1984. Morphology and internal structure of sandwaves in the Bay of Fundy. *Sedimentology*, 31(3), 365–382.

Dalrymple, R.W. and Rhodes, R.N., 1995. Estuarine dunes and bars. *In:* Perillo, G.M.E. (ed.), *Developments in Sedimentology*, Volume 53, *Geomorphology and Sedimentology of Estuaries*, Elsevier, pp. 359–422.

Doré, A.; Bonneton, P.; Marieu, V., and Garlan, T., 2016. Numerical modeling of subaqueous sand dune morphodynamics. *Journal of Geophysical Research: Earth Surface*, 121(3), 565–587.

Engel, P. and Lau, Y.L., 1981. Bed load discharge coefficient. *Journal of the Hydraulics Division*, 107(11), 1445–1454.

Engelund, F. and Fredsøe, J., 1982. Sediment ripples and dunes. *Annual Review of Fluid Mechanics*, 14(1), 13–37.

Exner, F.M., 1920. Zur physik der dunen. *Akademie der Wissenschaften in Wien/Mathematisch-Naturwissenschaftliche Classe*, 129(2a), 929–952.

Fredsøe, J. and Deigaard, R., 1992. *Mechanics of Coastal Sediment Transport*, Volume 3. *In:* Liu, P.L.-F. (ed.), *Advanced Series on Ocean Engineering*. Singapore: World Scientific, 392p.

Hoekstra, P.; Bell, P.; van Santen, P.; Roode, N.; Levoy, F., and Whitehouse, R., 2004. Bedform migration and bedload transport on an intertidal shoal. *Continental Shelf Research*, 24(11), 1249–1269.

Hopkins, J.; Elgar, S.; and Raubenheimer, B., 2017. Flow separation effects on shoreline sediment transport. *Coastal Engineering*, 125, 23–27.

Irish, J.; Lynch, J.; Traykovski, P.; Newhall, A., and Prada, K., 1998. A self-contained sector- scanning sonar for bottom roughness observations as part of sediment transport studies. *Journal of Atmospheric and Oceanic Technology*, 16(11), 1830–1999.

Johnson, D.W., 1916. Contributions to the study of ripple marks. *The Journal of Geology*, 24(8), 809–819.

Jones, K.R. and Traykovski, P., 2018. A method to estimate bedform height and asymmetry from a low-mounted sidescan sonar. *Journal of Atmospheric and Oceanic Technology*, 35, 893–910.

Kimball, P.; Bailey, J.; Das, S.; Geyer, R.; Harrison, T.; Kunz, C.; Manganini, K.; Mankoff, K.; Samuelson, K.; Sayre-McCord, T.; Straneo, F.; Traykovski, P., and Singh, H., 2014. The WHOI Jetyak: An autonomous surface vehicle for oceanographic research in shallow or dangerous waters. *Proceedings of 2014 IEEE/OES Autonomous Underwater Vehicles (AUV)* (Oxford, Mississippi), pp. 1–7.

Kostaschuk, R.; Shugar, D.; Best, J.L.; Parsons, D.R.; Lane, S.N.; Hardy, R.J., and Orfeo, O., 2008. Suspended sediment transport over a dune. *Proceedings of Marine Sand-wave and River Dune Dynamics III* (University of Leeds, UK), pp. 197–201.

Lefebvre, A.; Ernstsen, V.B., and Winter, C., 2013. Estimation of roughness lengths and flow separation over compound bedforms in a natural-tidal inlet. *Continental Shelf Research*, 61, 98–111.

Li, W.; Franklin, W.R.; Magalhães, S.V., and Andrade, M.V., 2014. Restricted bathymetric tracklines interpolation. *24th Fall Workshop on Computational Geometry* (Storrs Connecticut), https://wrf.ecse.rpi.edu/nikola/pubdetails/li-fwcg-2014.html

Lobo, F.; Maldonado, A., and Noormets, R., 2010. Large-scale sediment bodies and superimposed bedforms on the continental shelf close to the Strait of Gibraltar: Interplay of complex oceanographic conditions and physiographic constraints. *Earth Surface Processes and Landforms*, 35(6), 663–679.

Myrow, P.M.; Jerolmack, D.J., and Perron, J.T., 2018. Bedform disequilibrium. *Journal of Sedimentary Research*, 88(9), 1096–1113.

Nielsen, P., 1992. *Coastal Bottom Boundary Layers and Sediment Transport*. Singapore: World Scientific, 324p.

Off, T., 1963. Rhythmic linear sand bodies caused by tidal currents. *AAPG Bulletin*, 47(2), 324–341.

Perillo, M.M.; Best, J.L.; Yokokawa, M.; Sekiguchi, T.; Takagawa, T., and Garcia, M.H., 2014. A unified model for bedform development and equilibrium under unidirectional, oscillatory and combined flows. *Sedimentology*, 61(7), 2063–2085.

Reynaud, J.-Y. and Dalrymple, R.W., 2012. Shallow-marine tidal deposits. *In:* Davis, R.A., Jr., and Dalrymple, R.W. (eds.), *Principles of Tidal Sedimentology*, Dordrecht, The Netherlands: Springer, pp. 335–369.

Rubin, D.M. and McCulloch, D.S., 1980. Single and superimposed bedforms: A synthesis of San Francisco Bay and flume observations. *Sedimentary Geology*, 26(1–3), 207–231.

Simons, D.B.; Richardson, E.V., and Nordin, C.F., Jr., 1965. *Bedload Equation for Ripples and Dunes*. Washington, D.C.: U.S. Government Printing Office, *Geological Survey Professional Paper 462-H*, 9p.

Soulsby, R., 1997. *Dynamics of Marine Sands: A Manual for Practical Applications*. London: Thomas Telford, 272p.

Stommel, H. and Farmer, H.G., 1952. *On the Nature of Estuarine Circulation, Part I*. Woods Hole, Massachusetts: Woods Hole Oceanographic, *WHOI Technical Report 52-88*, 84p.

Ten Brinke, W.; Wilbers, A., and Wesseling, C., 1999. Dune growth, decay and migration rates during a large-magnitude flood at a sand and mixed sand–gravel bed in the Dutch Rhine River system. *In:* Smith, N.D. and Rogers, J. (eds.), *Fluvial Sedimentology VI*. Special Publication Number 28 of The International Association of Sedimentologists. Oxford, U.K.: Blackwell Science, pp. 15–32.

Venditti, J.G.; Church, M., and Bennett, S.J., 2005. Morphodynamics of small-scale superimposed sand waves over migrating dune bedforms. *Water Resources Research*, 41(10), W10423, 14p.

Winter, C.; Vittori, G.; Ernstsen, V., and Bartholdy, J., 2008. On the superimposition of bedforms in a tidal channel. *Proceedings of the 3rd International Workshop on Marine and River Dune Dynamics (MARID2008)* (Leeds, U.K.), pp. 337–344.